Aerodynamic Effects of Inviscid Parallel Shear Flows

M. H. Williams*
Princeton University, Princeton, N.J.
M. R. Chi†
NASA Ames Research Center, Moffett Field, Calif.
C. S. Ventres‡
Bolt Beranek and Newman Inc., Cambridge, Mass.
and
E. H. Dowell§
Princeton University, Princeton, N.J.

A general theory of planar disturbances in inviscid parallel shear flows, analogous to thin-wing theory in potential flows, has been developed. Integral relations between surface pressure and deformation are obtained that are similar to, and can be solved by the same numerical methods as those of potential flow. Computed results are shown that illustrate the effects of a model turbulent boundary layer on various lifting and nonlifting surfaces, including an elastic panel in low supersonic flow and an airfoil control surface in subsonic flow.

I. Introduction

THE methods of classical linearized potential flow theory have proved to be extraordinarily useful in the analysis of aeroelastic interactions, largely because of the existence of simple linear integral relations between deformation and induced force. In this paper, we consider the development and application of such relations for a class of nonpotential flows, namely inviscid, parallel shear flows, which are subjected to infinitesimal disturbances arising from the motion of a nearly plane surface. This theory has applications to such problems as the generation of waves at a free surface, the interaction of a boundary layer with a flexible wall, the flow about a wing in or near a jet or wake, and the influence of the main boundary layer of a wing on control surface effectiveness.

Specific results will be discussed for the following problems: 1) the wavy wall in a compressible turbulent boundary layer; 2) panel flutter in a low supersonic turbulent boundary layer; and 3) lifting surfaces in a velocity defect layer: a) steady rectangular wings (incompressible), b) two-dimensional steady airfoils (compressible), c) two-dimensional oscillating airfoils and flutter (incompressible), and d) two-dimensional control surfaces (steady compressible and unsteady incompressible).

II. Basic Relations and Assumptions

We assume that the fluid is an inviscid perfect gas which, in the absence of any disturbance, is described by the velocity, density, and pressure fields

$$u=\bar{u}(z), \quad v=w=0$$

$$\rho=\bar{\rho}(z)$$

$$p=p_\infty=\bar{\rho}(z)R\bar{T}(z) \tag{1}$$

The pressure must be constant to preserve momentum in the gradient z direction.

The flow (1) is disturbed by the infinitesimal motion of a thin body lying nearly in the plane $z=0$. The disturbance field, then, is governed by Euler's equations linearized about the mean flow (1). We apply the inviscid linearized boundary condition

$$w'=\left(\frac{\partial}{\partial t}+\bar{u}\frac{\partial}{\partial x}\right)f_\pm \text{ on } z=\pm 0 \tag{2}$$

where $z=f\pm(x,y,t)$ describes the position of the upper and lower surfaces of the body, w' is the perturbation velocity in the z direction, and x is the coordinate in the freestream direction. This surface constraint, together with the condition that all disturbances must decay as $x\to-\infty$ (upstream) and possible wake constraints (e.g., the Kutta condition) serve to determine the flowfield.

We seek a direct relation between the surface pressure disturbance $p'(x,y,\pm 0,t)$ and surface motion $f\pm(x,y,t)$. Because the governing equations are autonomous in x, y, t [the mean flow (1) depends only on z], such a relation can be found by superposition of wavy wall solutions (Fourier transforms in x,y).

Consider two infinite sinusoidal walls

$$z=f\pm(x,y,t)=F^*_\pm \exp(i\boldsymbol{k}\cdot\boldsymbol{x}-i\omega t) \tag{3}$$

where the surface $f+$ is exposed to the upper flow ($z>0$) and $f-$ to the lower flow ($z<0$). By linearity, we see that the induced surface pressures will be of the form

$$p(x,y;\pm 0,t)=P^*_\pm(\boldsymbol{k},\omega)\exp i\boldsymbol{k}\cdot\boldsymbol{x}-i\omega t \tag{4}$$

Moreover, the amplitudes P^* and F^* must be proportional. We express this proportionality in the conventional form

$$K^*_\pm(\boldsymbol{k},\omega)P^*_\pm(\boldsymbol{k},\omega)=w^*_\pm(\boldsymbol{k},\omega)=i(\alpha u_\infty-\omega)F^*_\pm \tag{5}$$

where α is the component of $\boldsymbol{k}$ in the x direction, u_∞ is a characteristic velocity (introduced for later convenience), and $K^*_\pm$ are the constants of proportionality to be determined. We note that $K^*_\pm$, which are admittance functions, are uniquely and independently determined by the upper and lower flows (1).

Received Jan. 21, 1977; presented as Paper 77-158 at the AIAA 15th Aerospace Sciences Meeting, Los Angeles, Calif., Jan. 24-26, 1977; revision received May 18, 1977.

Index categories: Aerodynamics; Nonsteady Aerodynamics.

*Research Associate, Department of Aerospace and Mechanical Sciences.

†NRC Research Associate.

‡Senior Research Scientist.

§Professor, Department of Aerospace and Mechanical Sciences.

The pressure fields induced by the wavy walls are governed by the differential equation (cf. Ref. 1)

$$M_\omega^2 (d/dz) M_\omega^{-2} (dp/dz) - k^2 (1 - M_\omega^2) p = 0 \tag{6}$$

where

$$k = |\boldsymbol{k}|$$

$$M_\omega (z;\boldsymbol{k},\omega) = [\bar{u}(z)\alpha - \omega]/[k\bar{a}(z)]$$

is the Mach number of the flow relative to the wave front. This equation was first derived by Lighthill[5] in a study of shock boundary-layer interactions. Equation (6) must be solved subject to the surface constraints

$$M_\omega^{-2} \frac{dp}{dz}\bigg|_{\pm 0} = k\gamma p_\infty f_\pm \tag{7}$$

and boundedness/radiation conditions at infinity (in an unbounded field) or appropriate outer wall constraints if the field is bounded by a plane surface. Methods for solving this boundary value problem are discussed in Ref. 1. The simplest numerical procedure is to convert Eq. (6) to a Riccatti equation

$$\frac{1}{k}\frac{dV}{dz} = M_\omega^{-2} - 1 - M_\omega^2 V^2 \qquad V \equiv \frac{1}{kM_\omega^2 p}\frac{dp}{dz} \tag{8}$$

which can be integrated directly from the outer fields (where V is known from the outer boundary conditions) to $z = \pm 0$. From the boundary condition (7) and the definition (5) of the admittance functions, it follows that

$$K_\pm^* (\boldsymbol{k},\omega) = i(\alpha u_\infty - \omega/\gamma p_\infty) V(\pm 0;\boldsymbol{k},\omega) \tag{9}$$

To obtain relations equivalent to Eq. (5) for a general surface configuration, we split the pressure and "upwash" into symmetric and antisymmetric parts

$$P_\pm^* = \bar{P}^* \pm \tfrac{1}{2}\Delta P^*, \qquad w_\pm^* = \bar{w}^* \pm \tfrac{1}{2}\Delta w^* \tag{10}$$

and solve Eq. (5) for the symmetric parts

$$\bar{w}^* = K^*\Delta P^* - L^*\Delta w^*$$

$$\bar{P}^* = L^*\Delta P^* + M^*\Delta w^* \tag{11}$$

where

$$K^* = K_+^* K_-^* / (K_-^* - K_+^*)$$

$$L^* = \tfrac{1}{2}(K_+^* + K_-^*)/(K_-^* - K_+^*)$$

$$M^* = 1/(K_+^* - K_-^*) \tag{12}$$

Superposition of Eqs. (11) yields a pair of integral relations between surface pressure and displacement for an arbitrary geometry. If the motion is simple harmonic in time and

$$w_\pm \equiv u_\infty (\partial f_\pm/\partial x) - i\omega f_\pm = \bar{w} \pm \tfrac{1}{2}\Delta w \tag{13}$$

then Eq. (11) reduces to:

$$K\vartheta\Delta p = \bar{w} + L\cdot\Delta w \tag{14}$$

$$\bar{p} = L\cdot\Delta p + M\cdot\Delta w \tag{15}$$

where K, L, M are integral operators of the form

$$U\cdot\phi = \int_S dx_1 \phi(x_1) U(x_1 - x;\omega) \qquad U = K,L,M \tag{16}$$

where

$$U(x_1;\omega) = \frac{1}{(2\pi)^{n-1}} \int_k d\boldsymbol{k} U^*(\boldsymbol{k};\omega)\exp(-i\boldsymbol{k}\cdot x_1) \tag{17}$$

and n is the dimension of the problem. The integral operators act only over the planform S of the surface since Δp and Δw must vanish off the surface.

If the shape of the surface is given, then Eq. (14) is an integral equation for the lifting pressure Δp and Eq. (15) gives the symmetric part of the pressure explicitly. We note that the lifting and nonlifting problems are in general coupled (one way) by the operator L. If the flow (1) is symmetric in z (as in a potential flow), then L vanishes. For a purely nonlifting problem we set $L = \Delta p = \bar{w} = 0$ so that

$$\bar{p} = M\cdot\Delta w \tag{18}$$

For a thorough exposition of the fundamental theory, the reader should consult Ref. 1.

III. Nonlifting Problems

In this section, we consider the interaction of a boundary layer on a flat plate with a local deformation of the plate surface. If the Reynolds number based on the characteristic wavelength of the deformation is large, but the growth of the (undisturbed) boundary layer over a wavelength is small, then the boundary-layer flow can be treated, locally, as an inviscid parallel shear flow. The surface pressure, therefore, is given by Eq. (18) where the integration spans the entire (x,y) plane and the kernel of M is determined by the local undisturbed boundary-layer profile.

For simplicity we shall suppose that the local profile is given by

$$\bar{u}(z)/u_\infty = (z/\delta)^{1/N} \qquad z \le \delta$$

$$\bar{T}(z)/T_\infty = 1 + (\gamma - 1)M_\infty^2 (1 - \bar{u}^2/u_\infty^2)/2 \tag{19}$$

which models a turbulent boundary layer of thickness δ under adiabatic conditions. It will be noted that this profile is invalid for $z \ll \delta$ since no attempt has been made to describe the laminar sublayer. For reasons discussed below this neglect is crucial to the success of the theory.

We first consider the interaction of the flow (19) with an infinite sinusoidal wall of wavelength $2\pi/\alpha$ in the flow direction. In the interest of clarity we consider only the two-dimensional, steady case, although three-dimensional, unsteady problems are not substantially more difficult to solve.

For any steady flow with $\bar{u}(0) = 0$ [as in Eq. (19)], the governing equation (6) of the wavy wall problem has a singularity at $z = 0$. This singularity is a consequence of the fact that the linearization invoked to obtain Eq. (6) cannot be valid near any point where $\bar{u} = 0$. Nevertheless, it can be shown that Eq. (6) does have a solution satisfying the far-field conditions and the surface constraint (7), provided that $\bar{u}(z)$ vanishes sufficiently slowly that $1/M_\omega^2 \sim 1/\bar{u}^2$ is integrable at $z = 0$ [this is apparent from Eq. (8)]. For the flow (19), this constraint limits consideration to values of $N > 2$. Since experimental observations of turbulent boundary layers indicate that $N \ge 7$ this limitation has little importance to the present considerations. However, it should be borne in mind that the simple linear inviscid theory given here cannot work for a laminar profile or for a turbulent profile with an accurate description of the laminar sublayer. For such problems, either nonlinear interactions or direct viscous forces (or both) must be included in the formulation. One of the consequences of the present work is that such refinements are not necessary for the turbulent case.

For *subsonic* external Mach numbers, the surface pressure, induced by the flow (19) on a steady two-dimensional wavy wall, varies with wavelength and Mach number as illustrated in Fig. 1 (from Ref. 1). The boundary layer always tends to reduce the pressure amplitude below its potential flow value (but with no shift in phase, theoretically). The decrease becomes more pronounced as $M_\infty \to 1$. At $M_\infty = 1$ the pressure remains finite for all nonzero δ.

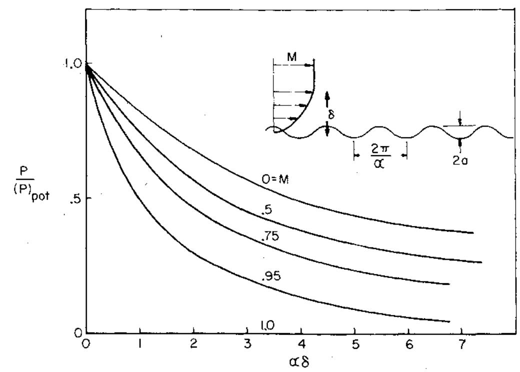

Fig. 1 Subsonic wavy wall pressure.

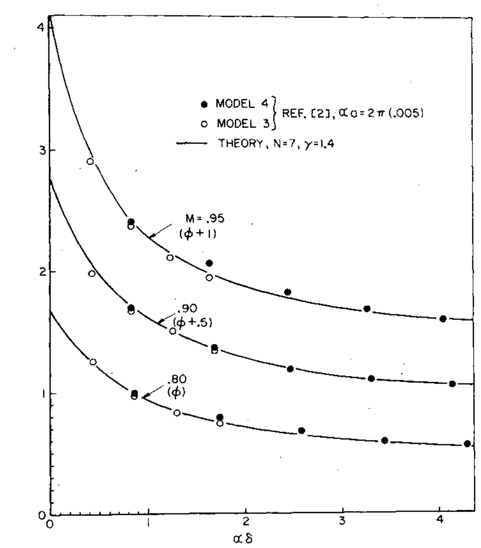

Fig. 2 Comparison of theory and experiment: subsonic wavy wall pressure $\phi \equiv |C_p|/(2\alpha a)$.

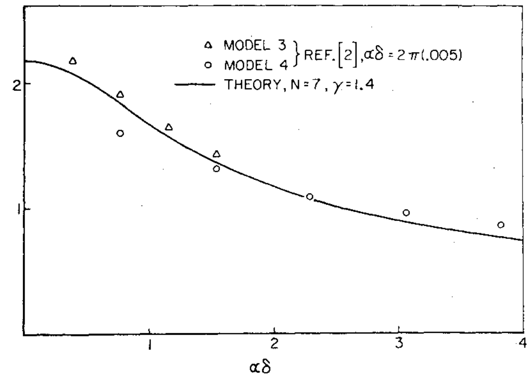

Fig. 3 Wavy wall pressure, $M = 1.1$, magnitude.

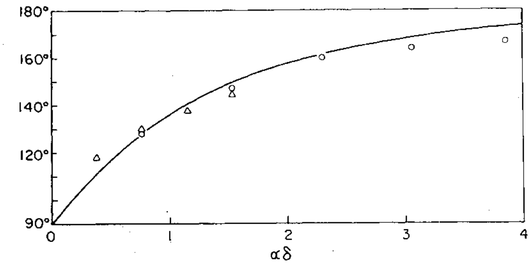

Fig. 4 Wavy wall pressure, $M = 1.1$, phase.

The above results are compared in Fig. 2 with the experimental results of Muhlstein and Beranek[2] at $M_\infty = 0.8$, 0.9, and 0.95. The comparisons are made by equating the theoretical and measured displacement thicknesses. The experimental data include only the fundamental spatial harmonic at the smallest amplitude to wavelength ratio (0.005) considered in Ref. 2. It is of some interest that according to potential flow theory the critical Mach number of this configuration is 0.92, although no distinct transonic phenomena are observed even at $M_\infty = 0.95$. The agreement between theory and experiment shown in Fig. 2 is remarkable considering the relatively crude boundary-layer profile used in the calculation. This fact suggests that a precise description of the undisturbed boundary-layer profile and, in particular an accurate modeling of the laminar sublayer, is not necessary for the quantitative prediction of surface pressure at wavelengths which are long compared to the laminar sublayer thickness.

In a *supersonic* external stream the boundary layer not only decreases the magnitude of the induced pressure, but also increases the phase lag toward 180°. These effects have been studied by Yates[3] using a formulation similar to that considered here but with an approximation valid for small $\alpha\delta$. The exact solution for the flow (19) at $M_\infty = 1.1$ is shown in Figs. 3 and 4. The measured results from Ref. 2 are, as in the subsonic case, in excellent agreement with the theory over the reported range of $\alpha\delta$.

As shown by Yates[3] for the supersonic case, and more generally in Ref. 1, the behavior of the solution for small $\alpha\delta$ is controlled by various integral properties of the boundary-layer profile. This fact is largely responsible for the close agreement shown in Figs. 2-4. However, the behavior of the solution for large $\alpha\delta$ is controlled by the structure of $\bar{u}(z)$ very near the surface. Thus the theory can be expected to be increasingly inaccurate as $\alpha\delta$ increases to large values, although both theory and experiment (if such existed) would show the pressure amplitude dropping to zero in this limit.

Three-dimensional and/or unsteady solutions to the wavy wall problem can either be computed directly,[4] or, in some cases, approximated from the two-dimensional steady solution. For instance, if the Strouhal number based on boundary-layer thickness $\omega\delta/u_\infty$ is small, then we can expect significant unsteady effect to arise only when $\alpha\delta \lesssim \omega\delta/u_\infty \ll 1$, i.e., for wavelengths that are long compared to δ. Conversely, at these wavelengths the boundary layer will have very little effect on the pressure. Thus a uniformly valid (for all α) approximation to the pressure at small $\omega\delta/u_\infty$ can be constructed from the steady *shear flow* and the *unsteady potential* flow solutions. This approximation is extensively developed in Ref. 6 for the incompressible case.

Similarly, the principal effect of three dimensionality (in the steady case) is to reduce the effective freestream Mach number. Thus, for instance, Fig. 1 can be interpreted as an approximate three-dimensional solution by taking the curves labeled "M_∞" to mean "$M_\infty \alpha/k$" and the abscissa to be $k\delta$. This relation would be exact for the flow (19) if $\gamma = 1$.

The pressures induced by an arbitrary wall deformation can be constructed from the wavy wall solution by simple superposition. This has been done for flexible rectangular panels in low supersonic streams and used in conjunction with an appropriate structural model to predict aeroelastic stability boundaries. The resulting flutter boundaries are shown in Figs. 5 and 6 (from Ref. 4), which illustrate the effect of boundary-layer thickness on flutter speed at $M_\infty = 1.2$ and of Mach number on flutter speed for fixed boundary-layer thickness. These results are compared to the stability boundaries determined experimentally in Ref. 7. The agreement is again quite good, although not as precise as in the wavy wall problem, presumably because of both numerical and experimental inaccuracies in this more complex physical situation.

The surface pressures found in the wavy wall problem determine, as shown in Sec. II, the admittance functions $K^*_\pm$

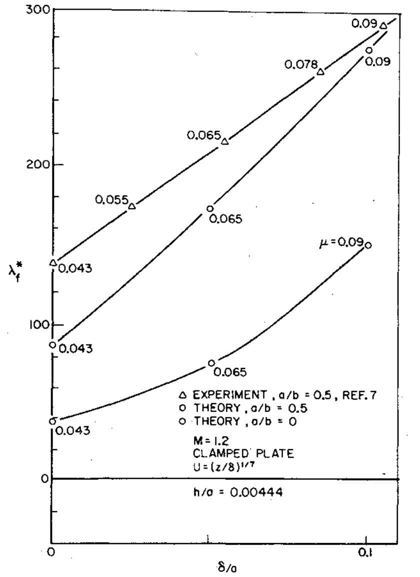

Fig. 5 Panel flutter dynamic pressure as function of shear layer thickness: $M=1.2$.

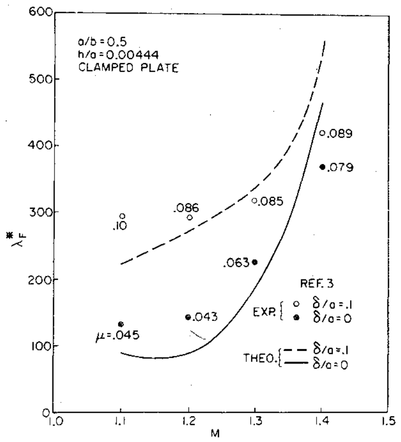

Fig. 6 Panel flutter dynamic pressure as function of M.

and thus the kernels for the general lifting surface problem. This topic will be considered in Sec. IV.

IV. Lifting Problems

We consider here several applications of the theory described in Sec. II to the evaluation of boundary-layer effects on lifting surfaces. To this end, we suppose that the undisturbed flow (corresponding to the flow over a flat plate at zero inclination) is given by Eq. (19) for both $z \gtrless 0$, as shown in Fig. 7. From symmetry, it follows that $K_+^* = -K_-^*$, so that

$$K^* = \tfrac{1}{2}K_+^* \qquad L^* = 0 \qquad M^* = 1/(2K_+^*) \tag{20}$$

where K_+^* is the admittance function of the upper flow. The lifting surface problem, then, becomes

$$\int_S \mathrm{d}x_1 K(x_1 - x)\Delta p(x_1) = \bar{w}(x) \equiv u_\infty \frac{\partial \bar{f}}{\partial x} - i\omega \bar{f} \tag{21}$$

where $\bar{f}$ is the displacement of the mean surface. We note that Eq. (21) is identical in form to the lifting surface problem in an unbounded potential flow and therefore can be solved using the same numerical techniques.

It must be emphasized that the flow illustrated in Fig. 7 is a highly idealized model of the real boundary layer and wake system associated with the undisturbed surface. Calculations based on this model, therefore, will at best give a qualitative

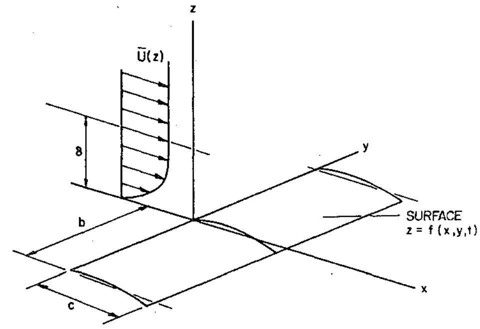

Fig. 7 Shear flow over a wing surface.

estimate of boundary-layer effects on the overall aerodynamic characteristics of a wing. Such overall effects, however, are generally very small, scaling roughly with the boundary-layer thickness to chord ratio. The principal practical application of the model is to the estimation of the relatively larger effect of the main wing boundary layer on trailing edge control surfaces. For such problems, the parallel flow assumption is approximately correct in the vicinity of the control surface. The approximation is better the smaller the control surface compared to the total planform. Correspondingly, the boundary layer will have a proportionately larger effect on the characteristics of the control surface in this limit. Thus, the model can be expected to be most accurate for those lifting problems for which it is most needed.

For the flow (19), the kernel K is of the form

$$K = \frac{1}{\delta^2}\bar{K}\left(\frac{x_1 - x}{\delta};\quad M_\infty, \frac{\omega\delta}{u_\infty};\ \gamma, N\right) \tag{22}$$

where $\bar{K}$ is a universal nondimensional function of its arguments. If δ is allowed to vanish, it can be shown that Eq. (22) approaches its potential flow form

$$K \to \left(\frac{\omega}{u_\infty}\right)\bar{K}_p\left(\frac{\omega}{u_\infty}(x_1 - x);\ M_\infty\right);\quad |x_1 - x| \gg \delta \tag{23}$$

This implies that the solution $\Delta p(x)$ of Eq. (21) will approach the potential flow solution (as δ vanishes) almost everywhere. The limiting pressure will differ significantly from its potential flow value within regions of width $\sim\delta$ near the boundaries of the planform S and near any lines of discontinuity of w (hinge lines). This behavior is in accord with experimental observation. However, since these nonuniformities occur over regions of vanishing measure the integral aerodynamic characteristics of the surface approach their potential flow values for small δ.

Because the assumed flow (19) is always subsonic near the surface, the kernel function (22) always has a "subsonic" strong algebraic singularity, whether $M_\infty \gtrless 1$. This implies that the solution of Eq. (21) is nonunique. The particular solution is chosen that satisfies that Kutta condition $\Delta p = 0$ on all trailing edges.

To investigate the effect of finite shear-layer thickness to chord ratio several calculations have been performed for the rigid body motions of simple wings (without control surface). These computations employed the method of collocation for the solution of Eq. (21). Only lift and moment results will be discussed here. Detailed results may be found in the cited references.

Figures 8 and 9 (from Ref. 8) show the lift curve slope and center of pressure (c.p.) on steady rectangular symmetric wings of varying aspect ratios in an incompressible flow. Because of the low momentum of the fluid near the surface, the shear layer induces a substantial decrease in the lift. However, only a very modest (downstream) shift is found in the c.p. This is a reflection of the fact that the shape of the

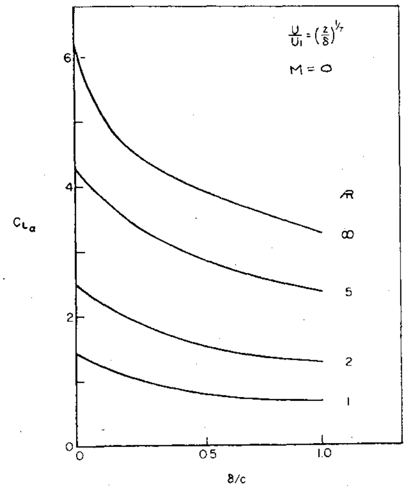

Fig. 8 Lift curve slope for rectangular wings, $M=0$.

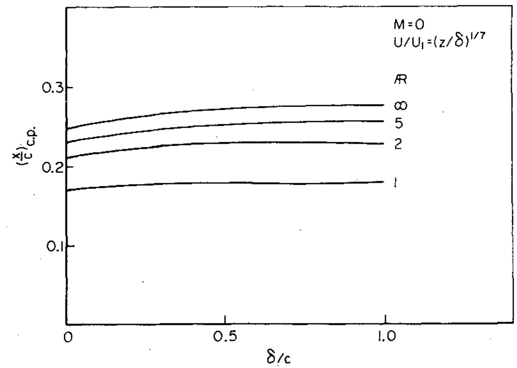

Fig. 9 Center of pressure for rectangular wings, $M=0$.

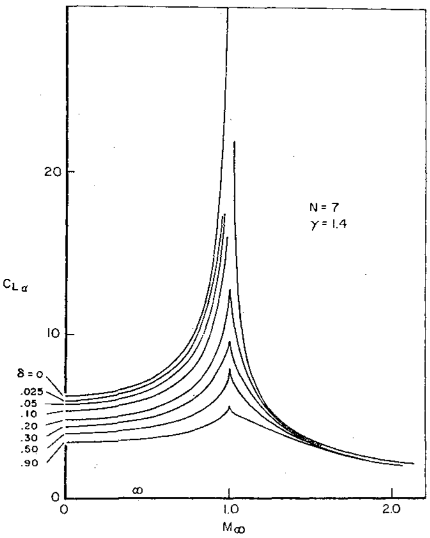

Fig. 10 Lift slope, compressible, steady, symmetric airfoils.

pressure distribution is changed only slightly by the shear layer. The aspect ratio has little influence on the relative changes in either lift or c.p. induced by the shear layer.

Compressibility effects have been investigated for steady symmetric airfoils. The lift slope and c.p. for this case are shown in Figs. 10 and 11 (from Ref. 1) as functions of M_∞ and δ/c. Not surprisingly, these results indicate a strong shear-layer effect, i.e., large deviations from the Prandtl-Glauert rule, near $M_\infty=1$. As in the wavy wall case, the solution to the lifting problem is bounded at $M_\infty=1$ for any nonzero δ. The lift decreases monotonically with δ/c at all

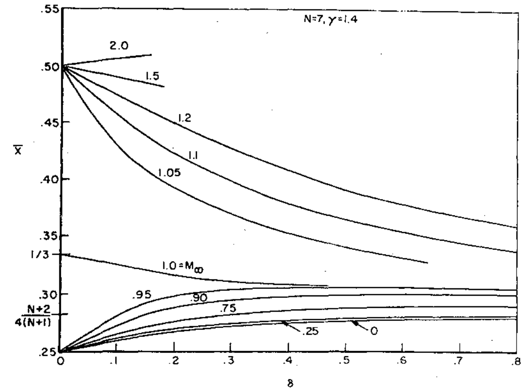

Fig. 11 Center of pressure, compressible, steady, symmetric airfoils.

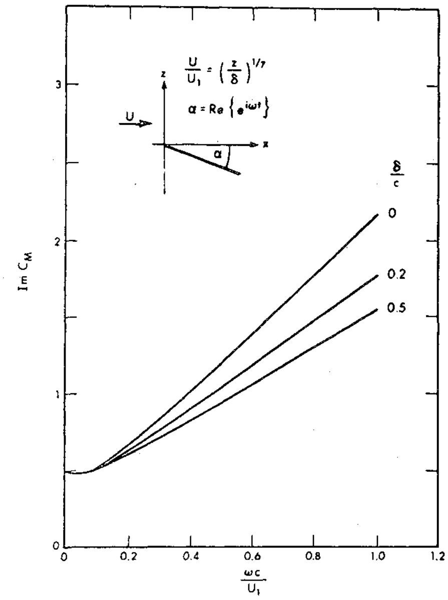

Fig. 12 Real part of pitching moment on airfoil oscillating about its leading edge, $M=0$.

Mach numbers, although this decrease becomes very weak for $M_\infty \geq 1.4$. Note, however, that the c.p. shifts are not monotonic and do not decrease with M_∞ in the supersonic regime.

For $1<M_\infty \lesssim 1.8$, the c.p. lies upstream from the mid-chord, whereas at larger M_∞ it lies downstream. This critical Mach number (~ 1.8) is identical to the critical Mach number discussed by Yates.[3]

Solutions have also been obtained for the pitching and heaving motions of an airfoil oscillating in an incompressible shear flow. These results are based on the kernel

$$K(x;\delta,\omega)=K(x;o,\omega)+K(x,\delta,o)-K(x;0,0) \qquad (24)$$

which is a composite of the steady shear flows and unsteady potential flow kernels. This approximation is valid for $\omega\delta/u_\infty \ll 1$, for reasons that were discussed in Sec. III. A complete description of the calculations will be found in Refs. 6 and 9.

Figures 12 and 13 show the real and imaginary parts of the pitching moment on an airfoil oscillating about its leading edge as a function of reduced frequency and shear-layer thickness. These results are typical in that they show a systematic decrease by the shear layer in both the in-phase and out-of-phase components of the reaction.

These pitching motion results, together with corresponding results for the heaving case, have been used to compute both single- and two-degree-of-freedom flutter boundaries. The

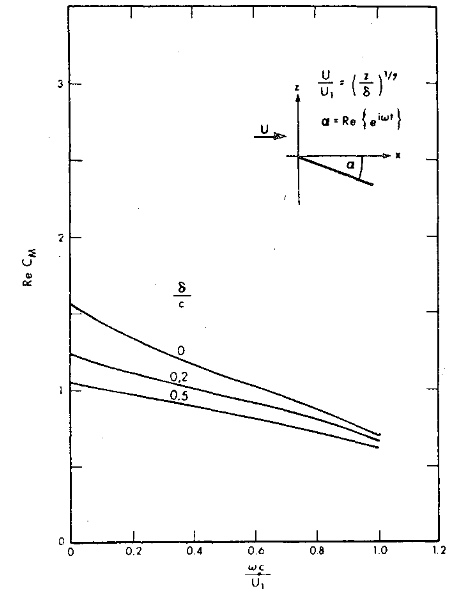

Fig. 13 Imaginary part of pitching moment on airfoil oscillating about its leading edge, $M=0$.

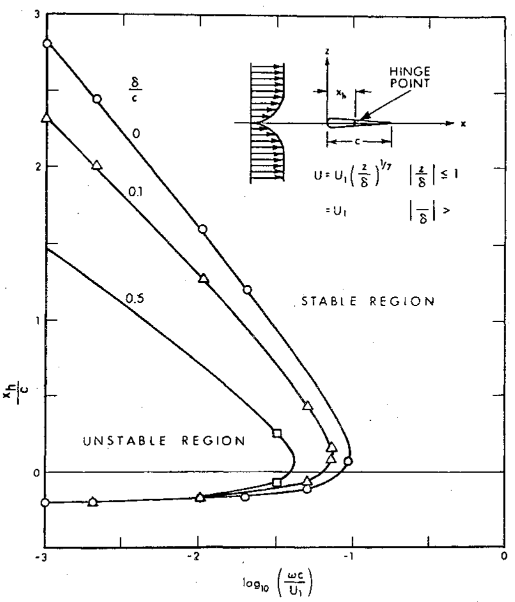

Fig. 14 Stability boundaries for single-degree-of-freedom flutter of an airfoil, $M=0$.

boundaries for simple rotation about a fixed axis are illustrated in Fig. 14 (from Ref. 9). It is apparent that the shear layer has a stabilizing influence in this case. This is also generally true for the two-degree-of-freedom problem (for a "typical section" airfoil as described in Ref. 10) as shown in Fig. 15 (from Ref. 6).

All of the aforementioned results are in qualitative agreement with experimental data in the sense that computed changes from potential flow theory are of the same sign as those that have been measured. Quantitative agreement (between the corrections to potential flow) is not found and should not be expected, both because of the mathematical approximations within the model and because the measured values involve many small contributions (e.g., nonlinearities, finite span effects, etc.) which cannot be accounted for.

The aerodynamic characteristics of trailing edge control surfaces (unlike those of full wings and airfoils) are typically predicted quite poorly by potential flow theory. It is plausible that this is largely due to the fact that such surfaces are not

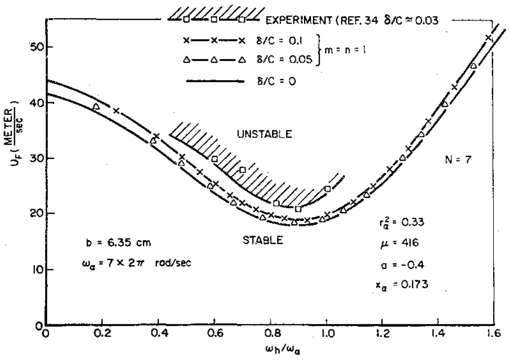

Fig. 15 Two-degree-of-freedom flutter speed, $M=0$.

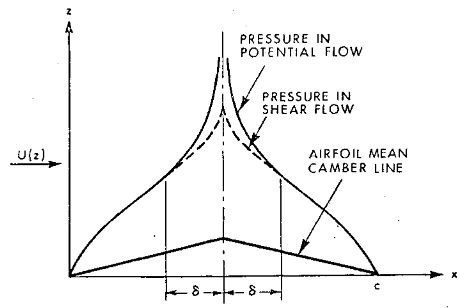

Fig. 16 Effect of shear on hinge singularity.

imbedded in a uniform flowfield but in the boundary layer flow generated on the main wing. We will now consider some results for a two-dimensional control surface imbedded in the flow (19), which represents the boundary layer formed on the main airfoil surface. It should be noted that a similar problem has been considered by Yates[11] using a two-layer potential flow model of the boundary layer and neglecting leading edge effects.

The discontinuity in downwash at the hinge line induces a singularity in the pressure, which, in a subsonic potential flow, is logarithmically infinite. For the flow (19), the pressure remains finite at the hinge (but with infinite gradient) as shown in Fig. 16. In either case, this behavior causes numerical difficulties in trying to solve the integral equations by the methods used earlier. Two techniques have been used to circumvent these difficulties.

The first method analytically constructs the solution for a control surface from the solutions of the simple airfoil problems found previously. This construction is based on the general solution, obtained in Ref. 12 of the integral equation (20) in the two-dimensional case. Specific results have been calculated for steady compressible flows.

The second method, which unlike the first can easily be extended to the three-dimensional case, is the so-called vortex lattice scheme. Specific results have been obtained for an oscillating control surface in an incompressible flow.

Figure 17 illustrates the variation of static hinge moment with hinge location and shear layer thickness at $M_\infty=0.75$. The moment coefficient is based on control surface chord and thus approaches a finite limit as $c_F/c \to 0$ according to potential flow theory. For any fixed $\delta/c>0$, however, the hinge moment must vanish as $c_F/c \to 0$ since the control surface then "sees" only the low momentum fluid within the shear layer. As expected, the relative effect of the shear layer is greatest for small c_F/c.

The variation in hinge moment with M_∞ at a fixed chord ratio $c_F/c=0.25$ is shown in Fig. 18. Also shown here are measured values (from Ref. 13) for a NACA 64A-006 airfoil with a quarter chord, sealed gap, flap.

We note that transonic effects dominate the flow above $M_\infty \sim 0.85$ (the critical Mach number for this airfoil). The

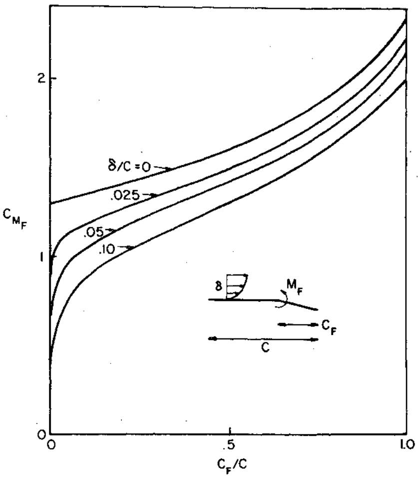

Fig. 17 Static hinge moment, $M = 0.75$.

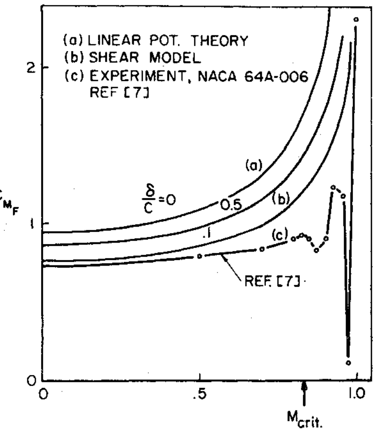

Fig. 18 Static hinge moment, $c_F/c = 0.25$.

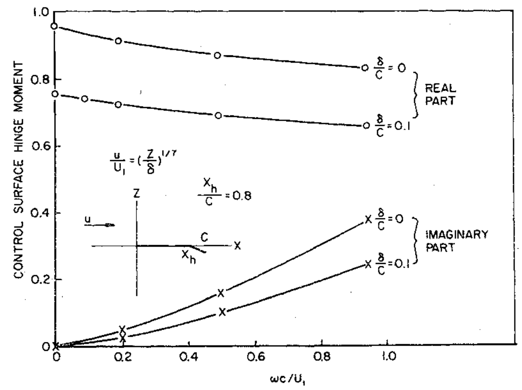

Fig. 19 Unsteady hinge moment, $M = 0$.

present theory cannot predict such phenomena. Below the critical Mach number the theory accounts for only a part of the difference between linear potential flow theory and measurement. As shown in Ref. 13, the inclusion of thickness effects (based on nonlinear potential flow computations) tends to reduce the calculated loading on the flap and thus the hinge moment. The calculated and measured results would thus be in better agreement if thickness effects were included.

Calculations for an oscillating flap have been restricted to the incompressible case. Figure 19 shows the hinge moment on a 20% chord oscillating flap as a function of reduced frequency. The shear layer has a larger influence (proportionally) on the out-of-phase component and can therefore be expected to have a substantial effect on dynamic stability.

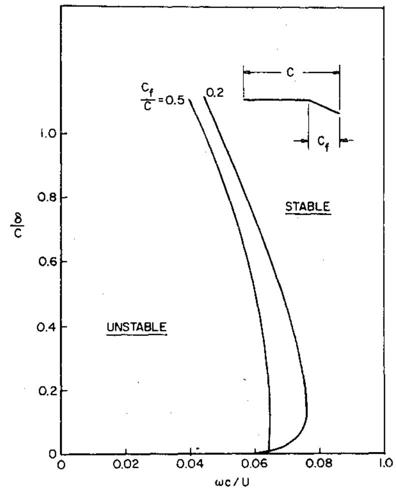

Fig. 20 Control surface flutter boundaries, $M = 0$.

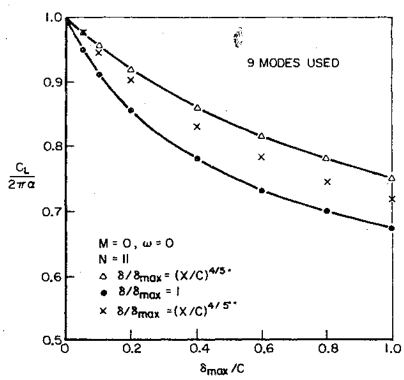

Fig. 21 Lift slope: effect of varying shear layer thickness, $M = 0$.

This is illustrated in Fig. 20 which shows the single degree-of-freedom flutter boundaries at two chord ratios. The shear layer has a distinctly destabilizing effect, especially at the smaller chord ratio, at small values of δ/c. The reason for this unexpected behavior is not clear.

V. Nonparallel Shear Flows

All of the above results, in both the lifting and nonlifting cases, were based on the assumption that the undisturbed flow does not vary in the x,y plane. If such nonuniformities are present, integral relations of the form (14-15) still exist (for infinitesimal disturbances) but the kernel functions depend on x and x_I separately rather than on $x-x_I$ alone (and, therefore, the kernels cannot be constructed from the wavy wall solution).

It was found, however, that for a shear layer of thickness δ the effect of the shear on the kernel functions is effectively confined to regions of width $|x-x_I| \sim \delta$ (at greater distances the kernels approach their potential flow forms). We now consider a shear layer that is nonuniform in the x,y directions, with thickness $\delta(x)$, say, that adjoins a uniform external potential flow, and that has gradients in the x,y directions that are small compared to the gradients in the z direction. The kernel function K can then be written in the nondimensional form

$$K(x,x_I) = \delta(x)^{-2}\bar{K}[(x_I - x)/\delta(x);\ x/L] \tag{25}$$

where $L = \|\nabla\delta/\delta\|^{-1} \gg \delta$ is the characteristic scale for variations in the x,y plane. As long as $\delta/L \ll 1$ it is reasonable to suppose that the function (25) can be computed by the methods discussed in Sec. III using the flow profile present at the point x/L. Thus for values $|x_I - x| \sim \delta$ the function (25) assumes its parallel shear flow form (peculiar to the point x/L,) whereas when $|x_I - x| \gg \delta$, it approaches the potential flow kernel (which is the same for all x/L).

Approximations of this type have been discussed in Ref. 14. A typical result is shown in Fig. 21 which compares the incompressible two-dimensional lift slope computed for constant δ to that for a shear-layer thickness varying like $x^{4/5}$. The profile at each chordwise position is presumed to be given by Eq. (19) with $N=7$. It should be noted that the slowly varying condition assumed in Eq. (25) is met only for $\delta/c \ll 1$.

VI. Conclusions

The general theory presented in Sec. III has been shown to predict accurately surface pressure loads induced by the interaction of a turbulent boundary layer with small local deformations of a plane surface. The simple boundary-layer profile (19) has been found to be adequate provided that the dominant wavelength of the deformation is not much smaller than the boundary-layer thickness. Excellent agreement with experiment has been shown for flow over a rigid wavy wall and good agreement obtained with panel flutter experiments.

The theory can be used to compute load distributions on lifting surfaces with about the same level of difficulty as that encountered in linearized potential flow calculations. Theoretical predictions of boundary-layer effects on lifting surfaces are in qualitative agreement with more elaborate calculation schemes (based on boundary-layer inviscid-flow matching) and with experiment. The quantitative validity of the results is still unclear in the absence of definitive experiments or systematic results from other theories. It is felt that the model should predict static and dynamic control surface moments, if nonlinear thickness effects are neligible. A proper evaluation of the theory requires either a means of calculating such nonlinearities or a carefully controlled set of experiments designed to isolate the influence of the boundary layer.

Acknowledgment

This work was supported by NASA grant 31-001-197 with NASA Ames Research Center.

References

[1] Williams, M. H., "General Theory of Thin Wings in Inviscid Parallel Shear Flows," Princeton University AMS Rept. 1269, March 1976.

[2] Muhlstein, L. and Beranek, R. G., "Experimental Investigation of the Influence of the Turbulent Boundary Layer on the Pressure Distribution over a Rigid Two-Dimensional Wavy Wall," NASA TN-D-6477, Aug. 1971.

[3] Yates, J. E., "Linearized Integral Theory of Three-Dimensional Unsteady Flow in a Shear Layer," *AIAA Journal*, Vol. 12, May 1974, pp. 596-601.

[4] Dowell, E. H., "Generalized Aerodynamic Forces on a Flexible Plate Undergoing Transient Motion in a Shear Flow with an Application to Panel Flutter," *AIAA Journal*, Vol. 9, May 1971, pp. 834-841.

[5] Lighthill, M. J., "On Boundary Layers and Upstream Influence, II; Supersonic Flows without Separation," *Proceedings of the Royal Society*, Vol. A 217, May 1953, pp 478-507.

[6] Chi, M. R., "Unsteady Lifting Surface Theory in an Incompressible Shear Flow," Princeton University AMS Rept. No. 1283, Oct. 1976.

[7] Muhlstein, L., Gaspers, P. A., and Riddle, D. W., "An Experimental Study of the Influence of the Turbulent Boundary Layer on Panel Flutter," NASA TN-D-4486, March 1968.

[8] Ventres, C. S., "Shear Flow Aerodynamics: Lifting Surface Theory," *AIAA Journal*, Vol. 13, Sept. 1975, pp. 1183-1189.

[9] Ventres, C. S., "Nonsteady Shear Flow Lifting Surface Theory," Bolt, Beranek and Newman Inc., Rept. 3235, Jan. 1976.

[10] Bisplinghoff, R. L., Ashley, H., and Halfman, R. L., *Aeroelasticity*, Addison-Wesley, Reading, Mass., 1957.

[11] Yates, J. E., "Pressure Distribution on the Trailing Edge of an Airfoil Oscillating in a Shear Layer," ARAP Rept. No. 278, April 1976.

[12] Williams, M. H., "The Resolvent of Singular Integral Equations," *Quarterly of Applied Mathematics*, April 1977, pp 99-110.

[13] Tijdeman, H., "High Subsonic and Transonic Effects in Unsteady Aerodynamics," NLR TR 75079 U, May 1975, National Aerospace Laboratory, Netherlands.

[14] Chi, M. R., "Steady Incompressible Variable Thickness Shear Layer Aerodynamics," *AIAA Journal*, Vol. 14, Sept. 1976, pp. 1155, 1156.